



## Original Research Article

# MicroRNA-29a-5p attenuates hemorrhagic transformation and improves outcomes after mechanical reperfusion for acute ischemic stroke

Chang-Luo Li<sup>a,b,c,1</sup>, Jin-Kun Zhuang<sup>a,b,c,1</sup>, Zhong Liu<sup>b,d</sup>, Zhong-Run Huang<sup>a,b,c</sup>,  
Chun Xiang<sup>a</sup>, Qian-Yu Chen<sup>b,c</sup>, Ze-Xin Chen<sup>b,c</sup>, Zhong-Song Shi<sup>a,b,c,e,\*</sup> 

<sup>a</sup> Department of Neurosurgery (C-LL, J-KZ, Z-RH, CX, Z-SS), Sun Yat-sen Memorial Hospital, Sun Yat-sen University, Guangzhou, China

<sup>b</sup> RNA Biomedical Institute (C-LL, J-KZ, ZL, Z-RH, Q-YC, Z-XC, Z-SS), Sun Yat-sen Memorial Hospital, Sun Yat-sen University, Guangzhou, China

<sup>c</sup> Nanhai Translational Innovation Center of Precision Immunology (C-LL, J-KZ, Z-RH, Q-YC, Z-XC, Z-SS), Sun Yat-sen Memorial Hospital, Sun Yat-sen University, Foshan, China

<sup>d</sup> Department of Neurosurgery (ZL), Zhongshan Hospital of Xiamen University, School of Medicine, Xiamen University, Xiamen, China

<sup>e</sup> Guangdong Province Key Laboratory of Brain Function and Disease (Z-SS), Sun Yat-sen University, Guangzhou, China



## ARTICLE INFO

## Keywords:

Acute ischemic stroke  
Hemorrhagic transformation  
Cerebral ischemia-reperfusion injury  
Oxygen-glucose deprivation reoxygenation  
MicroRNA  
Astrocyte

## ABSTRACT

**Background:** Hemorrhage transformation (HT) following endovascular reperfusion treatment is associated with worse clinical outcomes in acute ischemic stroke patients. MicroRNA (miR) modulates several aspects of cerebral ischemia-reperfusion injury, including blood-brain barrier (BBB) integrity, inflammation, oxidative stress, and apoptosis, significantly impacting cerebral recovery and function. This study investigated the role of astrocytic miR-29a-5p in HT in the transient middle cerebral artery occlusion (MCAO) model and oxygen-glucose deprivation reoxygenation (OGD/R) model of astrocytes.

**Methods:** MiR-29a-5p expression in the OGD/R astrocyte model was assessed. The astrocyte injury, the expression of A1 and A2 phenotypes of reactive astrocytes, and the regulation of miR-29a-5p target genes were evaluated after the miR-29a-5p intervention. A mechanical reperfusion-induced HT model was established in hyperglycemic rats using 5-h MCAO following reperfusion at 6 h. MiR-29a-5p agomir was administered intravenously before reperfusion. Infarct volume, HT, BBB damage, neurological score, the expression of miR-29a-5p, and its target genes were evaluated.

**Results:** MiR-29a-5p expression decreased in OGD/R-treated astrocytes and the peri-infarction tissue and blood of the MCAO model. Elevating miR-29a-5p levels reduced astrocyte injury, suppressed neurotoxic A1 astrocyte markers (C3, Fkbp5, and Serpin1), while enhanced neuroprotective A2 astrocyte markers (S100a10 and Emp1) in the OGD/R and MCAO models. Intravenous administration of miR-29a-5p agomir increased the expression of miR-29a-5p and reduced infarct volume, reperfusion-induced HT, and BBB breakdown after ischemia, improving neurological outcomes in the MCAO model. Overexpression of miR-29a-5p effectively suppressed the expression of its direct target genes, glycogen synthase kinase 3 beta and aquaporin 4 in the OGD/R and MCAO models.

**Conclusions:** MiR-29a-5p alleviates astrocyte injury and regulates A1 and A2 astrocyte markers, glycogen synthase kinase 3 beta, and aquaporin 4 in astrocytes subjected to ischemia-reperfusion injury. Astrocytic miR-29a-5p may be a protective target for reducing HT and improving outcomes following mechanical reperfusion in acute ischemic stroke.

## 1. Introduction

Acute ischemic stroke (AIS) patients with intracranial large-vessel

occlusion can benefit from earlier treatment with endovascular thrombectomy and intravenous alteplase [1–3]. However, the cerebral ischemia-reperfusion injury that often follows reperfusion treatments

Peer review under the responsibility of Editorial Board of Non-coding RNA Research.

\* Corresponding author. Department of Neurosurgery, Sun Yat-sen Memorial Hospital, Sun Yat-sen University, 107 Yanjiang West Road, Guangzhou, Guangdong, China.

E-mail address: [shizhs@mail.sysu.edu.cn](mailto:shizhs@mail.sysu.edu.cn) (Z.-S. Shi).

<sup>1</sup> CLL and JKZ have contributed equally to this work.

<https://doi.org/10.1016/j.ncrna.2025.05.016>

Received 13 February 2025; Received in revised form 17 May 2025; Accepted 28 May 2025

Available online 28 May 2025

2468-0540/© 2025 The Authors. Publishing services by Elsevier B.V. on behalf of KeAi Communications Co. Ltd. This is an open access article under the CC BY license (<http://creativecommons.org/licenses/by/4.0/>).

introduces new challenges, including hemorrhagic transformation (HT) and exacerbated inflammatory responses, which are detrimental to recovery and are predictive of poor long-term outcomes in AIS patients [4–8]. Emerging research has highlighted the pivotal role of non-coding RNAs in these processes. MicroRNA (miR) modulates several aspects of cerebral ischemia-reperfusion injury, including blood-brain barrier (BBB) integrity, inflammation, oxidative stress, and apoptosis, significantly impacting cerebral recovery and function [9–14].

The miR-29 family, including miR-29a, miR-29b, and miR-29c, is significantly downregulated in cerebral ischemia-reperfusion injury, which affects cellular responses to ischemic damage [15–18]. Specifically, miR-29a-5p influences neuroglial interactions, impacting microglial activation and glutamate release and affecting the volume of ischemic damage and infarcts seen in animal stroke models [19]. Studies suggest that nicotinamide adenine dinucleotide phosphate oxidase inhibitor, by increasing miR-29a-5p levels, help to reduce cerebral infarct volumes and HT after reperfusion in ischemic rat tissues [20,21]. By regulating these key processes, miR-29a-5p plays a pivotal role in reducing the detrimental effects of ischemia-reperfusion injury and promoting neuroprotection. Non-coding RNAs, including microRNAs, have emerged as important diagnostic and prognostic blood biomarkers for AIS due to their stability in body fluids and specific expression patterns in response to ischemic injury [9,10,14]. MiR-29a-5p was found to be significantly downregulated in the plasma of stroke patients, correlating with the severity of brain injury and clinical outcomes [19]. This makes miR-29a-5p a valuable biomarker for early diagnosis and prognosis, aiding in the prediction of patient outcomes and the personalization of therapeutic strategies.

Astrocytes, the predominant type of glial cells in the central nervous system, play critical roles in supporting neuronal function and contributing to neurodegenerative processes [22]. In ischemic stroke, reactive astrocytes can adopt a neurotoxic A1 phenotype or a neuroprotective A2 phenotype. A1 astrocytes exacerbate neuronal damage by releasing pro-inflammatory cytokines and reactive oxygen species, while A2 astrocytes promote recovery by secreting neurotrophic factors and anti-inflammatory cytokines [23,24].

MiR-29a is highly expressed in astrocytes. Despite its protective roles, the function of miR-29a-5p in HT remains inadequately understood. This study aims to clarify the mechanisms by which astrocytic miR-29a-5p regulates HT using the oxygen-glucose deprivation and reoxygenation (OGD/R) model and a mechanical reperfusion-induced HT model in hyperglycemic rats. The focus is on how miR-29a-5p influences the expression between neurotoxic A1 astrocytes, which can exacerbate injury, and neuroprotective A2 astrocytes, which aid recovery. By understanding the interactions between miR-29a-5p and its target genes within astrocytes, this study aims to uncover novel molecular mechanisms that could be targeted to reduce HT following endovascular reperfusion treatment, offering the potential of miR-29a-5p as a therapeutic target in stroke treatment.

## 2. Materials and methods

### 2.1. Establishing a mechanical reperfusion-induced HT model in hyperglycemic rats

The experimental protocol received approval from our institution's Institutional Animal Care and Use Committee. Adult male Sprague-Dawley rats (8–10 weeks, 250–280 g) were utilized to establish a hyperglycemia-associated reperfusion-induced HT model following established protocols [20,21,25,26]. The intraluminal filament technique was performed to have the left middle cerebral artery occlusion (MCAO) for 5 h, followed by reperfusion at 6 h. Anesthesia was initiated with 5 % isoflurane in a 70 % nitrogen/30 % oxygen mixture and maintained with 2 % isoflurane via a facemask. Body temperature was stabilized at 37.0 °C using a heating pad. Immediate reperfusion was achieved by filament withdrawal after the ischemic period. Animals

were euthanized 6 h post-reperfusion (11 h post-ischemia onset) for tissue collection.

Acute hyperglycemia was induced through intraperitoneal administration of 50 % dextrose (6 mL/kg) 15 min pre-occlusion, maintaining blood glucose >16.7 mmol/L. Sustained hyperglycemia during ischemia was achieved via supplemental 50 % dextrose injections (1.5 mL/kg) at 1, 2, 3, and 4 h post-MCAO. Blood glucose monitoring occurred via tail vein sampling at baseline and 0.5, 1, 2, and 4 h post-dextrose administration. The hyperglycemic condition increases the extent of cerebral hemorrhage after ischemia-reperfusion in a rat model with 5-h MCAO.

### 2.2. MiR-29a-5p agomir administration in HT model

In the study, 151 rats met the criteria of successful surgery and acute hyperglycemia. One rat was excluded because of subarachnoid hemorrhage after the surgery. First, 30 hyperglycemic rats were used to assess the dynamic analysis of the levels of miR-29a-5p in the peri-infarction tissue and whole blood. Rats were randomly enrolled into five groups: sham group, 5-h MCAO following reperfusion at 0, 1, 3, and 6 h (6 rats per group).

Then, rats were used to assess the role of miR-29a-5p in HT and the underlying mechanisms. One hundred and twenty hyperglycemic rats were randomly assigned into four groups: (1) sham-operated, (2) ischemia-reperfusion, (3) ischemia-reperfusion and microRNA control, (4) ischemia-reperfusion and miR-29a-5p agomir group (30 rats per group). Rats received an intravenous injection of miR-29a-5p agomir or microRNA control (Gene Pharma) at a dose of 50 nmol/kg body weight 30 min before reperfusion. Rats were sacrificed 6 h after reperfusion, and brains were harvested for the measurements.

Ischemic hemisphere peri-infarct regions were dissected using previously described methods [27]. Specifically, after delineating the midline separating the ischemic and non-ischemic hemispheres, a longitudinal incision was made along the sagittal plane, 2 mm lateral to the midline, extending from the top to the bottom across each hemisphere. Subsequently, an oblique transverse incision was made to divide the brain tissue into the infarction core (striatum and upper cerebral cortex) and the peri-infarct region (adjacent cerebral cortex). The peri-infarct tissue was used for further RT-PCR and Western blot study. The whole blood was collected and stored in the PAXgene Blood RNA tube (Pre-AnalytiX GmbH) to extract the total RNA.

### 2.3. Neurological evaluation

Neurological assessments were conducted pre-ischemia and 6 h post-reperfusion using a 5-point scale (0 = no neurological deficits; 1 = failure to extend contralateral forepaw fully; 2 = reduced resistance to lateral push; 3 = spontaneous circling to contralateral side; 4 = absence of spontaneous movement or unconsciousness).

### 2.4. Cerebral infarction quantification

Infarct volumes were determined via 2,3,5-triphenyl tetrazolium chloride (TTC) staining 11 h post-ischemia. Six 2-mm coronal sections were incubated with 2 % TTC solution (Sigma) for 20 min at room temperature. Edema-corrected infarct volume was calculated using ImageJ software as the following formula: (contralateral hemisphere volume – non infarct ipsilateral hemisphere volume)/contralateral hemisphere volume.

### 2.5. BBB integrity assessment

Evans blue extravasation was evaluated 11 h after ischemia. Evans blue solution (Sigma) was administered via the tail vein 8 h after ischemia. Three hours later, vascular clearance via cardiac perfusion preceded brain dissection. Hemispheric samples were homogenized in trichloroacetic acid, centrifuged (10,000 g, 30 min), and

spectrophotometrically analyzed at 620 nm.

Evans blue extravasation index was expressed as the ratio of absorbance intensity in the ischemic hemisphere to that in the non-ischemic hemisphere.

## 2.6. Measurement of cerebral hemorrhage

Cerebral hemoglobin content was measured spectrophotometrically 11 h post-ischemia. Homogenized hemispheric samples in PBS were centrifuged (13,000 g, 30 min), mixed with Drabkin's reagent (Sigma), and analyzed by spectrophotometry at 540 nm. The hemoglobin content index was calculated as hemoglobin content in the ipsilateral hemisphere divided by that in the contralateral hemisphere.

## 2.7. Astrocyte cell culture and OGD/R model

Primary astrocytes were isolated from neonatal Sprague-Dawley rat cortices as previously reported [28]. The cortex was isolated and then digested with 0.25 % trypsin (Gibco, 25200072) at 37 °C for 20 min. The digestion was terminated with a complete medium containing DMEM-F12 (Gibco, C11330500B), 10 % FBS (Gibco, 10099141), and 1 % Penicillin-Streptomycin (Gibco, 15140122). The cell suspension was collected using a 70 µm nylon cell filter and centrifuged at 1000 rpm for 5 min. Cells were resuspended using the complete medium, plated into 75 cm<sup>2</sup> flasks, and then cultured in a humidified incubator with 5 % CO<sub>2</sub> at 37 °C, with the complete medium replaced every 2–3 days. We identified the purity of astrocytes using immunofluorescence and used the third-generation cells to perform the subsequent OGD/R experiments.

Astrocytes underwent OGD/R in hypoxic chambers (Stemcell) (95 % N<sub>2</sub> and 5 % CO<sub>2</sub>, Stemcell) with glucose-free medium (Gibco, 11966025) for 6 h, followed by normoxic reoxygenation in glucose-containing complete medium. We collected the cells 0, 3, 6, 12, and 24 h after reoxygenation. Astrocytes did not receive OGD as the control.

## 2.8. Prediction of hub target genes for miR-29a-5p

The predicted target genes of miR-29a-5p were identified using the miRDB and TargetScan databases. We performed Kyoto Encyclopedia of Genes and Genomes (KEGG) pathway and Gene Ontology functional enrichment analyses to identify the biological functions of the predicted target genes using DAVID Bioinformatics Resources [29]. The predicted genes from the top ten most enriched KEGG pathways were used to search for the interactions of the target genes using the STRING tool. We obtained the protein-protein interaction network and investigated the top twenty hub genes using CytoHubba.

## 2.9. Transfection of miR-29a-5p mimics and inhibitors

Astrocytes were transfected with miR-29a-5p mimics and inhibitors, small interfering RNA (siRNA) for the predicted target gene, including glycogen synthase kinase 3 beta (Gsk3b), aquaporin 4 (Aqp4), and FKBP prolyl isomerase 5 (Fkbp5). The optimal concentrations of the miR-29a-5p mimics and miR-29a-5p inhibitors were 50 nM and 100 nM. The optimal sequence of siRNA for target gene of rat Gsk3b was as follows: sense strand: GGGAGCAAUUAGAGAAUUTT, antisense strand: AUUUCUCUAAUUUGCUCCTT. The optimal sequence of siRNA for target gene of rat Aqp4 was as follows: sense strand: GCACACGAAA-GAUCAGCAUTT, antisense strand: AUGCUGAUCUUUCGUGUGCTT. The optimal sequence of siRNA for target gene of rat Fkbp5 was as follows: sense strand: GUAUCUUGGACCACAAUUAUTT, antisense strand: AUAUUGUGGUCCAAGAUACTT. The miR-29a-5p mimics and inhibitors were synthesized by RiboBio. siRNA genes were synthesized by Gene Pharma.

Astrocytes were performed OGD/R and divided into six groups: blank control, OGD/R, OGD/R receiving negative control microRNA,

OGD/R receiving the miR-29a-5p mimics, OGD/R receiving the miR-29a-5p inhibitors, and siRNA gene (Gsk3b, Aqp4 and Fkbp5). Astrocytes were transfected with siRNA using Lipofectamine 3000 (Invitrogen, L3000015). After 48 h of incubation, OGD/R was performed, and then RT-PCR was performed to evaluate the transfection efficacy.

## 2.10. Cell counting Kit-8 (CCK-8) assay

A CCK-8 assay was used to detect the viability of cells in the OGD/R astrocyte model. Astrocytes were seeded into 96-well plates (5 × 10<sup>4</sup> cells/well) and then transfected with miR-29a-5p mimics (50 nM), miR-29a-5p inhibitors (100 nM), or negative control microRNA. After 48 h of incubation, 20 µL of CCK-8 solution (Dojindo Laboratories, CK04, Japan) was added to each well and incubated for 1 h. The absorbance of each well was measured at 450 nm.

## 2.11. Lactate dehydrogenase (LDH) assay

An LDH Cytotoxicity Colorimetric Assay Kit was used to analyze LDH release in the medium in the OGD/R astrocyte model. Astrocytes were divided into control, OGD/R, OGD/R receiving microRNA control, OGD/R receiving miR-29a-5p mimics, and OGD/R receiving miR-29a-5p inhibitors group. We collected and centrifuged the supernatants of each group. The LDH levels in supernatants were measured using an LDH Cytotoxicity Assay Kit (Beyotime Biotechnology, C0016, China). We measured the absorbance of each group at 490 nm to determine the LDH activity after 30 min of incubation.

## 2.12. Quantitative RT-PCR

The total RNA of the astrocytes in the OGD/R model and the peri-infarction tissue and whole blood in the MCAO model were extracted using a Trizol reagent (Invitrogen). The mRNAs of genes from the prediction analysis, A1 reactive astrocyte markers [complement C3 (C3), Fkbp5, serpin family G member 1 (Serping1), glycoprotein alpha-galactosyltransferase 1 (Ggta1), guanylate binding protein 2 (Gbp2)], and A2 reactive astrocyte markers [S100 calcium binding protein A10 (S100a10), pentraxin 3 (Ptx3), sphingosine-1-phosphate receptor 3 (S1pr3), epithelial membrane protein 1 (Emp1), CD109 molecule (Cd109)] were assessed. We used the SYBR green real-time RT-PCR and the TaqMan stem-loop method to assess the level of miR-29 and mRNA [20,21]. Quantitative RT-PCR was performed using the Applied Biosystem PCR System. We normalized the levels of mRNA and miR-29 family using β-actin and U6 as internal controls and used the 2-ΔΔCT method to calculate them. Each sample was tested in triplicate. The primers were designed and synthesized by RiboBio, China. The primer sequences are shown in Table 1.

## 2.13. Western blot

We extracted the total protein of the astrocytes following OGD/R and the peri-infarction tissue of the MCAO model using a bicinchoninic acid protein assay and assessed the levels of GSK3β, AQP4, FKBP5, and occludin. The anti-GSK3β (Abcam, ab131356, 1:1000), anti-AQP4 (Abcam, ab9512, 1:1000), anti-FKBP5 (Abcam, ab126715, 1:1000), and anti-occludin (Abcam, ab31721, 1:1000) antibodies were visualized using an HRP-conjugated secondary antibody and enhanced chemiluminescence. The expression bands of the protein were detected using a molecular imager system. The density of bands was normalized to β-actin (Abcam, ab227387, 1:1000). Each sample was tested in triplicate. Image J software was used to quantify the optical density value of proteins.

## 2.14. Dual-luciferase reporter assay

Dual-luciferase activity technology was used to clarify the

**Table 1**  
Sequences of the primer for mRNAs used in the qRT-PCR.

Primer name	Primer sequence	Length
C3	Forward: 5'AATTTATACCTTCCTCCGCCT3' Reverse: 5'GGAGTCCTTCACATCCACCC3'	104
Fkbp5	Forward: 5'ACGAGCCGTTGTCTTAGCC3' Reverse: 5'GCAGAGCCGTAAGCGTATTCT3'	127
Serping1	Forward: 5'ACGCTCTCTGAGCCTGTATG3' Reverse: 5'ACCCAGGTGTTGATGAGTTTAAAG3'	85
Ggta1	Forward: 5'TTCTGAACCTCACCAGGGAGT3' Reverse: 5'GGGATAGGATTTAGTGGGTTTGT3'	132
Gbp2	Forward: 5'GTCCTTCAAAAACCTAAATCCCATC 3' Reverse: 5'AAAGTTCAAGACACACTGCCATAG3'	76
S100a10	Forward: 5'ACAAAGGAGGACCTGAGAGTGC3' Reverse: 5'CTTTCAATTATTTTCCACAGCCAG3'	94
Ptx3	Forward: 5'ATTCTGCTTTGTGCTCTCTGGT3' Reverse: 5'GAAGTCCATTGTCTATTTCGTTGTC3'	100
S1pr3	Forward: 5'GAGACACCGTATACATTTACAGC3' Reverse: 5'GTGGACAACGTGACGAGCTT3'	93
Emp1	Forward: 5'CTATCTGGTTATGGAGCACTAAGCA3' Reverse: 5'CTTTATTCATCTCACAACTGCGT3'	99
Cd109	Forward: 5'CACAGTTCTGGTTGTATCGACA 3' Reverse: 5'TCCCTCAGGAACATGGTGCT3'	120
Wnt2b	Forward: 5'CCTTCCTCCACCTCAATCC3' Reverse: 5'CCTCTCTAGGGCTAAGGAACCGA3'	105
Wnt 3	Forward: 5'ACCTCCCACGGCATTGATG3' Reverse: 5'CAGTGGAAAGACGCAATGACATTT3'	101
Wnt 4	Forward: 5'TGCTCGGACAACATCGCT3' Reverse: 5'CTTGTCTCTCTCGGACG3'	70
Wnt5a	Forward: 5'GAGATTGTGGATCAGTTCGTGTG3' Reverse: 5'TAAATATGTGGTTCCTGGGAGTG3'	79
Wnt7b	Forward: 5'TGTCCAAGGTCAACGCAATG3' Reverse: 5'AGGGAGGTGATCCTCAGAGTCT3'	112
Wnt9b	Forward: 5'TACGCTATGACACGGCTGTCAA3' Reverse: 5'TGGGAGAATCTCCATGTAGACC3'	147
Wnt 16	Forward: 5'TGCAGAAGCCAGTTCCGACA3' Reverse: 5'CGCTACTCAGTTCATAGCAA3'	104
Fzd1	Forward: 5'CCGTGCGAACCCTAAAGTA3' Reverse: 5'TAGGTACGTGAGCACCGTGAA3'	132
Fzd2	Forward: 5'CAGGAGGAGACTCGTTTGGCC3' Reverse: 5'TCTGGGTAGCGGAATCGCT3'	119
Fzd3	Forward: 5'CAGCGTGCCTATAGTGAAGTCT3' Reverse: 5'GCTCATCAACAATCTGGAAACCTAC3'	97
Fzd4	Forward: 5'GTACACGGTTCCTGCGACCT3' Reverse: 5'GCCACGAGCAAAGACATAAA3'	136
Fzd8	Forward: 5'GCAGATTCTCTCGGCA3' Reverse: 5'AGGGCTCTACGGTGAGGAAC3'	88
Lrp6	Forward: 5'TGTGGTAGAGTTCCGGCTTAGATT3' Reverse: 5'ACCTCAATGCGATTGTTCCT3'	99
Dvl3	Forward: 5'GTCACCTTGGCGGACTTAAAG3' Reverse: 5'GCTTGGCATTGTTCATCCGA3'	118
Gsk3b	Forward: 5'ATCGCACTGTGTAGCCGTCT3' Reverse: 5'TTGGGTCCCGTAATTCAATAA3'	100
Ctnnb1	Forward: 5'AAGTCTTGGCTATTACGACAGACT3' Reverse: 5'AGCTTCTGCTAGCTGTAGTTCTC3'	134
Ptpn11	Forward: 5'CAGTATTGGTCTCCTCACTTGCC3' Reverse: 5'TGACCATGTTGCCAATCTCC3'	116
Egf	Forward: 5'TTGATAGCCGACAACACAC3' Reverse: 5'CGACTCTCAGTCTCTTGGCG3'	86
Aqp4	Forward: 5'TCGCCAAGTCCGCTTCTACA3' Reverse: 5'CGTGGTGACTCCCAATCCTC3'	113
Hgf	Forward: 5'GAGGTACGCTACGAAGTCTGTGA3' Reverse: 5'TGCCTGATTCTGTGTGATCCA3'	106
Kdr	Forward: 5'TCAGACGACACAGATACCACCG3' Reverse: 5'CCTGCAACATCCACCAGCTT3'	71
β-actin	Forward: 5'CGAGTACAACCTTCTTGACGC3' Reverse: 5'ACCCATACCCACCATCACAC3'	202

relationship between miR-29a-5p and Gsk3b and Aqp4. HEK 293T cells were seeded into 24-well plates, and X-tremegene HP (ROCHE) was used to transfect the plasmid. MiR-29a-5p mimics were transfected into HEK 293T cells with wild-type and mutant Gsk3b 3'UTR-carrying luciferase. A Passive Lysis Buffer was added to the well to lyse cells. The Luciferase Assay Reagent (Promega) was used to test firefly luminescence. Stop & Glo Reagent was used to test Renilla luminescence. The effect of miR-29a-5p on the activity of the Gsk3b luciferase reporter gene was

observed. In addition, dual-luciferase activity technology was used to clarify the relationship between miR-29a-5p and Aqp4 as the above method.

### 2.15. Statistical analysis

Statistical analyses were conducted using SPSS 30.0. All measurement data were expressed as mean ± standard deviation. The Shapiro-Wilk test was used to determine whether econometric data were normally distributed. One-way analyses of variance followed by the Least Significant Difference were performed to compare among three or more groups. The level of significance was set at 0.05.

## 3. Results

### 3.1. Increased miR-29a-5p alleviated astrocyte injury and regulated the expression of A1 and A2 phenotypes of reactive astrocytes in the OGD/R model

In OGD/R-treated astrocytes, there was decreased expression of miR-29a-5p at 24 h. The miR-29a-5p mimics increased the expression of miR-29a-5p in astrocytes following OGD/R, while miR-29a-5p inhibitors decreased the expression of miR-29a-5p (Fig. 1A). The miR-29a-5p mimics alleviated the astrocyte damage caused by CCK-8 ( $p < 0.001$ ), inhibited LDH release from astrocytes ( $p = 0.001$ ) in OGD/R-treated astrocytes. The miR-29a-5p inhibitors worsened cell damage ( $P < 0.01$ ) induced by OGD/R (Fig. 1B and C). The dynamic expression of the A1 reactive astrocyte markers (C3, Fkbp5, Serping1, Ggta1, Gbp2) and A2 reactive astrocyte markers (S100a10, Ptx3, S1pr3, Emp1, Cd109) following OGD at 0, 3, 6, 12, and 24 h after reoxygenation was shown in Supplementary Fig. S1. The expression of the A1 markers of C3, Fkbp5, and Serping1 was decreased ( $p < 0.001$ ), while the expression of the A2 markers of S100a10, Ptx3, and Emp1 was increased ( $p < 0.01$ ) after intervention with miR-29a-5p mimics compared to the OGD/R-treated group in astrocytes (Fig. 1D and E). It seems that upregulated miR-29a-5p can alleviate astrocyte injury, suppress A1-type astrocyte expression, and promote the activation of A2-type astrocytes after OGD/R.

### 3.2. Increased miR-29a-5p regulated the expression of predicted target genes for miR-29a-5p in the OGD/R model

Predicted target genes for miR-29a-5p were identified and were analyzed for biological function. The enriched KEGG pathways of the predicted target gene were revealed by DAVID Bioinformatics Resources (Supplementary Fig. S2A). Then, we selected 245 predicted targeted genes in the top ten KEGG pathways to establish the protein-protein interaction network (Supplementary Fig. S2B). The top twenty hub genes were identified (Fig. 2A and Supplementary Table S1). We found twelve hub genes with significantly differential expression in the astrocyte OGD/R model. Five hub genes were significantly upregulated 24 h after OGD/R, including Wnt family member (Wnt) 4, Wnt2b, frizzled class receptor (Fzd) 4, Fzd8, and Gsk3b. Seven hub genes were significantly downregulated 24 h after OGD/R, including β-catenin, Wnt5a, lipoprotein receptor-related protein 6 (Lpr 6), Fzd2, Fzd3, disheveled segment polarity protein (Dvl) 3, and hepatocyte growth factor (Supplementary Fig. S3).

MiR-29a-5p mimics suppressed the expression of Gsk3b and increased the expression of Fzd2 and Dvl3 among the twelve predicted hub genes in OGD/R-treated astrocytes ( $p < 0.01$ ) (Fig. 2B). The other nine predicted hub genes were not significantly regulated after intervention with miR-29a-5p mimics or inhibitors.

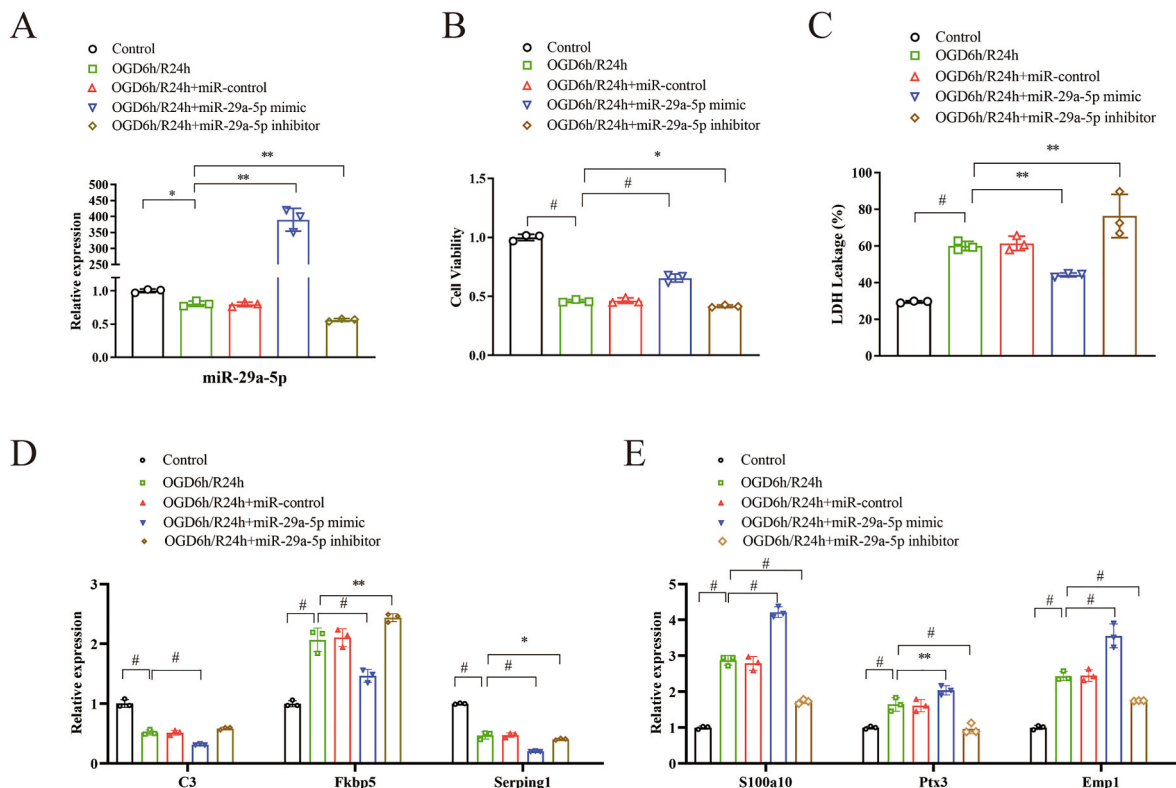


**Fig. 1.** Elevating miR-29a-5p levels was protective in ischemia-reperfusion injury in the OGD/R astrocyte model. **A**, miR-29a-5p mimics increased the expression of miR-29a-5p in astrocytes following OGD/R. **B**, miR-29a-5p mimics alleviated cell damage shown by CCK-8 assay. **C**, miR-29a-5p mimics inhibited LDH release from astrocytes. **D** and **E**, miR-29a-5p mimics decreased the expression of neurotoxic A1 reactive astrocyte markers (C3, Fkbp5, and Serping1) while increasing the expression of neuroprotective A2 reactive astrocyte markers (S100a10, Ptx3, and Emp1). Each sample was tested in triplicate. \* $P < 0.05$ ; \*\* $P < 0.01$ ; # $P < 0.001$ .

### 3.3. MiR-29a-5p regulated the expression of GSK3 $\beta$ , FKBP5, and AQP4 in the OGD/R model

MiR-29a-5p mimics suppressed the upregulated expression of GSK3 $\beta$  in OGD/R-treated astrocytes shown by Western blot analysis ( $p < 0.001$ ). Silencing the Gsk3b gene weakened the effect of the miR-29a-5p inhibitors on the expression of GSK3 $\beta$  in the astrocyte OGD/R model (Fig. 2C). MiR-29a-5p mimics suppressed the upregulated expression of FKBP5 in OGD/R-treated astrocytes ( $p < 0.01$ ). Silencing the Fkbp5 gene weakened the effect of the miR-29a-5p inhibitors on the expression of FKBP5 in the astrocyte OGD/R model (Fig. 2D). MiR-29a-5p mimics suppressed the upregulated expression of AQP4 in OGD/R-treated astrocytes ( $p < 0.001$ ). Silencing the Aqp4 gene weakened the effect of the miR-29a-5p inhibitors on the expression of AQP4 in the astrocyte OGD/R model (Fig. 2E).

### 3.4. Gsk3b and Aqp4 are the direct target gene for miR-29a-5p

The inhibitory effect of miR-29a-5p mimics on the target gene Gsk3b 3'UTR and Aqp4 3'UTR were detected using the dual-luciferase reporter assay. Site-specific mutagenesis technology determined the site of interaction between miR-29a-5p and Gsk3b 3'UTR. The miR-29a-5p mimics significantly inhibited the luciferase activity expressed in tandem with the wild-type Gsk3b 3'UTR ( $P < 0.001$ ) and partially inhibited the luciferase activity expressed in tandem with the mutant Gsk3b 3'UTR; however, the inhibitory ability was partially weakened. These results indicated that Gsk3b is a direct target gene for miR-29a-5p (Fig. 2F).

Site-specific mutagenesis technology determined the site of interaction between miR-29a-5p and Aqp4 3'UTR. The miR-29a-5p mimics significantly inhibited the luciferase activity expressed in tandem with the wild-type Aqp4 3'UTR ( $P < 0.001$ ). These results indicated that Aqp4

is a direct target gene for miR-29a-5p (Fig. 2G).

### 3.5. Increased miR-29a-5p regulated the expression of miR-29a-5p, A1 and A2 astrocyte markers in the hyperglycemia-associated reperfusion-induced HT model

The levels of miR-29a-5p were decreased in both the peri-infarction tissue and whole blood following reperfusion at 0 and 6 h in the rat MCAO model (Fig. 3A). Intravenous administration of miR-29a-5p agomir before reperfusion increased the expression of miR-29a-5p in both the peri-infarction and whole blood compared with the ischemia-reperfusion group ( $P < 0.001$ ) (Fig. 3B).

The mRNA expression of the A1 astrocyte markers (C3, Fkbp5, and Serping1) was decreased, while the expression of the A2 astrocyte markers (S100a10 and Emp1) was increased in the peri-infarction tissue after intervention with miR-29a-5p agomir (Fig. 3C).

### 3.6. Increased miR-29a-5p reduced infarct volume, HT, BBB breakdown, and improved functional outcome

MiR-29a-5p agomir treatment before reperfusion reduced cerebral infarct volume (TTC staining, 15.7 % versus 34.7 %,  $p < 0.001$ ) (Fig. 4A) and reduced HT (hemoglobin content index, 1.4 versus 1.9,  $p = 0.001$ ) (Fig. 4B), compared with the ischemia-reperfusion group in the rat MCAO model. There was less Evans blue extravasation after miR-29a-5p agomir treatment (1.9 versus 3.7,  $p < 0.001$ ), indicating the protection of BBB by increased the level of miR-29a-5p (Fig. 4C). Rats treated with miR-29a-5p agomir showed better neurological scores following reperfusion at 6 h (1.1 versus 2.2,  $p < 0.001$ ).



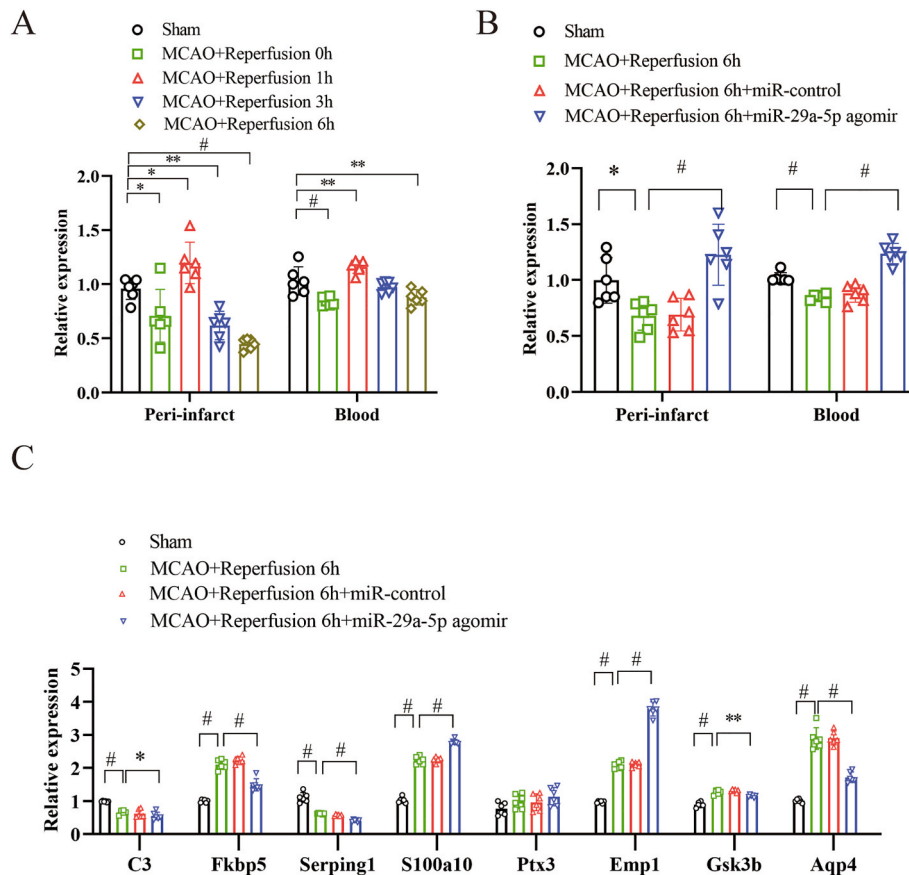


**Fig. 3.** Elevating miR-29a-5p levels regulated the expression of miR-29a-5p, predicted target genes, and A1/A2 astrocyte markers in the hyperglycemia-associated reperfusion-induced HT model. **A**, miR-29a-5p expression decreased in the peri-infarction tissue and blood of the MCAO model (n = 6). **B**, miR-29a-5p agomir treatment before reperfusion reduced the miR-29a-5p expression in the peri-infarction tissue and blood of the MCAO model (n = 6). **C**, miR-29a-5p agomir treatment suppressed the mRNA expression of A1 markers (C3, Fkbp5, and Serping1), Gsk3b, and Aqp4, while enhanced A2 markers (S100a10 and Emp1) in the peri-infarction tissue (n = 6). \*P < 0.05; \*\*P < 0.01; #P < 0.001.

### 3.7. Increased miR-29a-5p regulated the expression of GSK3 $\beta$ , FKBP5, AQP4, and occludin in the hyperglycemia-associated reperfusion-induced HT model

The mRNA expression of Gsk3b and Aqp4, as the direct target gene for miR-29a-5p, was decreased in the peri-infarction tissue after intervention with miR-29a-5p agomir (Fig. 3C). In addition, miR-29a-5p agomir treatment suppressed the increasing expression of GSK3 $\beta$ , FKBP5, and AQP4 in the peri-infarction tissue compared with the ischemia-reperfusion group (p < 0.001), as shown by Western blot analysis. The tight junction protein occludin expression was suppressed in the peri-infarction tissue after ischemia-reperfusion, whereas miR-29a-5p agomir treatment partly restored its expression, as shown by Western blot analysis (Fig. 4D).

## 4. Discussion

Our study provides novel evidence supporting the relationship between astrocytic miR-29a-5p and HT in ischemic stroke using an *in vitro* astrocyte OGD/R model and a hyperglycemia-associated reperfusion-induced HT rat model. The miR-29 family is significantly downregulated in cerebral ischemia-reperfusion injury, influencing cellular responses to ischemic damage [15–18]. Specifically, miR-29a-3p has been observed to decrease in the CA1 region in a rat forebrain ischemia model, where it targets the pro-apoptotic protein PUMA, thus mitigating ischemic injury in astrocytes and neurons *in vitro* [15,30]. Additional research has shown that miR-29a-3p overexpression protects neuronal cells from OGD/R injury by downregulating Rock1 and modulating TNFRSF1A and

NF- $\kappa$ B signal pathways [31,32]. MiR-29a-5p was found to be reduced in the plasma of stroke patients, correlating with the severity of brain injury and clinical outcomes. Knocking out miR-29a resulted in the increased M1 microglia polarization, thereby increasing infarct volume in a rat stroke model [19]. Collectively, these findings align with our results, suggesting that miR-29a-5p overexpression may reduce cerebral infarction volume, mitigate BBB disruption and HT, and improve functional outcomes in ischemic stroke models.

Our findings show that miR-29a-5p overexpression can attenuate astrocyte injury, decrease expression of neurotoxic A1 markers (C3, Fkbp5, and Serping1), and increase neuroprotective A2 markers (S100a10 and Emp1) following OGD/R and mechanical reperfusion after MCAO. These results suggest that miR-29a-5p promotes a neuroprotective environment that supports neuronal survival and tissue repair. In ischemic stroke contexts, reactive astrocytes can adopt either an A1 phenotype, associated with neurotoxicity and increased pro-inflammatory cytokine release, or an A2 phenotype, linked with neuroprotection and the secretion of neurotrophic and anti-inflammatory factors [23,24]. Increased S100a10 expression, a hallmark of A2 astrocytes, has shown protective effects in cerebral ischemia-reperfusion injury [33]. Moreover, the astrocyte-specific Kruppel-like factor 4 has been shown to suppress A1 activation and promote A2 polarization post-ischemia, primarily through NF- $\kappa$ B pathway modulation [24]. Research underscores that promoting the A2 phenotype can enhance post-stroke recovery by supporting neuronal survival and reducing inflammation [22,33]. Our results on the ability of miR-29a-5p to modulate astrocyte phenotypes add to this growing body of evidence, suggesting potential therapeutic strategies for reducing HT and

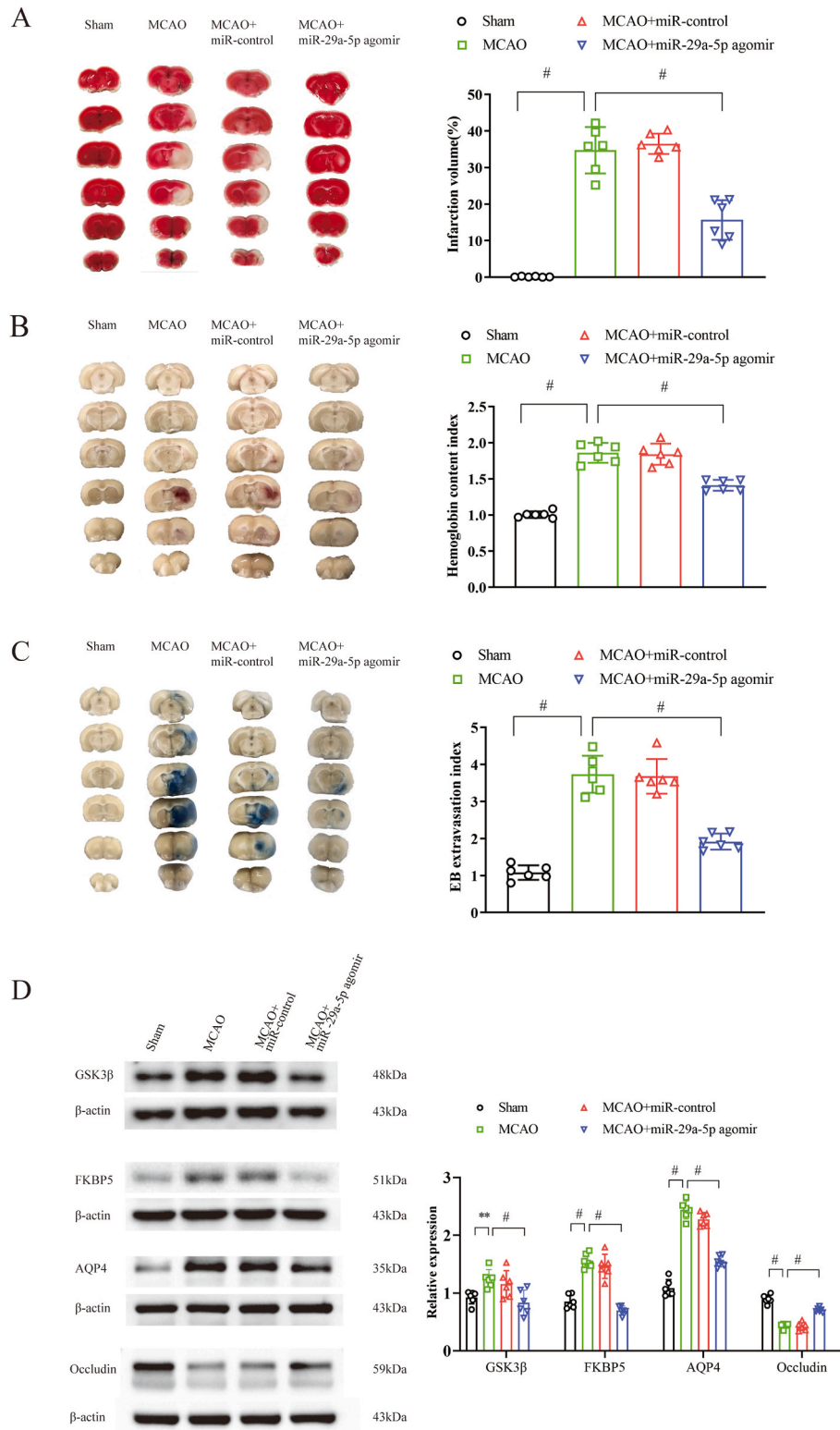


**Fig. 4.** MiR-29a-5p agomir reduces infarct volume, reperfusion-induced hemorrhage, and BBB disruption and improves neurological outcomes via regulating GSK3β, FKBP5, and AQP4. **A**, TTC staining of brain slices and quantification for infarct volume (n = 6). **B**, Hemoglobin content index is determined by spectrophotometric hemoglobin assay (n = 6). **C**, BBB permeability in the ischemic hemisphere was shown by Evans blue staining (n = 6). **D**, Western blot shows the expression of GSK3β, FKBP5, AQP4, and occludin in the peri-infarction tissue (n = 6). \*\*P < 0.01; #P ≤ 0.001.

improving post-stroke outcomes.

This study also reveals that increasing miR-29a-5p levels effectively downregulates its direct and predicted target gene *in vitro* and *in vivo*, illustrating its protective role in astrocytes. Our results indicate that

miR-29a-5p exerts this neuroprotection by regulating genes such as Gsk3b, Aqp4, and Fkbp5. Prior studies suggest that Gsk3b inhibition can protect the BBB and alleviate ischemia-reperfusion injury in ischemic stroke models [34]. Wnt-3a protein administration leads to Gsk3b

dephosphorylation, reducing cerebral infarction and neuronal apoptosis through the Foxm1 pathway [35]. Aqp4, an astrocyte endfeet marker, is upregulated in ischemic tissue following BBB disruption [36]. Notably, miR-29b overexpression has been shown to reduce BBB disruption in ischemic stroke by downregulating Aqp4 [16]. Nicotinamide adenine dinucleotide phosphate oxidase inhibitor has been found to decrease brain edema and HT by downregulating Aqp4 in the reperfusion-induced HT model [20]. We also identified Fkbp5 as a predicted target gene for miR-29a-5p. In a previous study, Fkbp5 was upregulated in cerebral ischemia-reperfusion injury and regulated autophagy via the AKT/FOXO3 signaling pathway [37]. In our study, we observed increased Fkbp5 levels in OGD/R-treated astrocytes and peri-infarction tissue of the HT model, which were reduced by miR-29a-5p overexpression.

Maintaining the integrity of BBB after ischemic and hemorrhagic brain injuries is crucial for reducing neurological impairment. Astrocytes, essential components of the BBB, help regulate its integrity and function through communication with endothelial cells and pericytes. Recent studies have indicated that reactive astrocytes, which vary in their responses to stroke damage, can harm or protect BBB integrity depending on their specific subsets [38,39]. In a mouse model of ischemic stroke, A1 reactive astrocytes induced by stroke disrupted BBB integrity, while blocking the conversion of A1 reactive astrocytes reduced BBB disruption [40]. In a mouse model of hemorrhagic stroke, there was an increase in inflammatory reactive astrocytes and the expression of inflammation-related genes. Notably, the matrix metalloproteinase-3 (MMP3), which is associated with BBB disruption, was significantly upregulated in these inflammatory reactive astrocytes. These astrocytes led to a reduction in the endothelial tight junction proteins ZO-1 and claudin-5. Inhibiting the MMP3 secreted by reactive astrocytes mitigated the loss of these tight junction proteins [41]. These findings suggest that inflammatory reactive astrocytes are crucial in driving BBB disruption during stroke. Conversely, astrocytes secrete Sonic hedgehogs that regulate the expression of endothelial tight junction proteins to maintain the integrity of the BBB [42]. In ischemic and hemorrhagic strokes, astrocytic Sonic hedgehog production is increased in the injured brain. This rise in production enhances tight junction proteins, specifically ZO-1 and claudin-5, which alleviate BBB permeability [43,44]. In our rat model of HT, enhancing the expression of astrocytic miR-29a-5p through a miR-29a-5p agomir protected BBB disruption, partly by restoring the tight junction protein occludin.

MicroRNAs are pivotal regulators of gene expression, with distinct 5p and 3p variants arising from the same precursor hairpin. The seed region differs between 5p and 3p, directing distinct target mRNA interactions. The isoforms of 5p and 3p have a functional divergence. MiR-21-3p and miR-21-5p have different roles in BBB injury after traumatic brain injury (TBI). Both microRNAs significantly increase shortly after TBI. However, they affect BBB damage differently [45–47]. Intraventricular infusion of miR-21-5p agonists boosts miR-21-5p levels in damaged brains, improving neurological function after TBI. Its protective effects activated the Ang-1/Tie-2 pathway and inhibited Caspase-9, thus reducing BBB leakage and secondary damage [45,46]. Conversely, elevated miR-21-3p in the early stages of TBI worsens BBB damage. Using miR-21-3p inhibitors decreases its expression in endothelial cells after TBI. These inhibitors target the gene methionine adenosyltransferase 2B, suppressing apoptosis and inflammation through the NF- $\kappa$ B pathway, reducing loss of tight junction proteins and BBB leakage while improving neurological function in TBI mice [47]. Such divergence highlights the need to study both isoforms to understand microRNA functionality. Relative levels of isoforms can shift with cellular conditions, disease states, or developmental stages. We found decreased expression of miR-29a-3p, miR-29a-5p, miR-29c-3p, and miR-29c-5p in OGD/R-treated astrocytes. MiR-29a-5p had the highest decreased expression among the six microRNAs of the miR-29 family (Supplementary Fig. S4). Research has demonstrated the significance of miR-29a-3p in astrocytes and its protective role in cerebral ischemia

[15,48–51]. These findings indicate that miR-29a-3p differentially regulates cell survival in hippocampal astrocytes, specifically between the CA1 region and the dentate gyrus, while alleviating OGD/R injury [48, 49]. Increasing the levels of miR-29a-3p using mimics has been shown to prevent brain damage and behavioral deficits in neonatal mice subjected to hypoxia-ischemia [50]. Additionally, miR-29a-3p in astrocyte-derived extracellular vesicles has been found to mitigate cerebral ischemia-reperfusion injury by downregulating TP53INP1 and the NF- $\kappa$ B/NLRP3 signaling pathway [51]. In various studies related to non-alcoholic steatohepatitis, resistance to Adriamycin in breast cancer, and ischemic injury, Gsk3b and Aqp4 have been identified as direct target genes of miR-29a-3p [49,52,53]. The distinction between transcripts is important for understanding the complexity of microRNAs. Their different biogenesis, target interactions, and roles in disease underscore the need for isoform-specific research to enhance therapeutic and diagnostic innovations.

Our study has certain limitations. Neurobehavioral function was not assessed in this study during the acute stage of stroke. The modified neurological severity score, rotarod, and corner tests provide composite measurements of motor skills, sensory function, reflexes, and balance. These assessments are more effective for evaluating neurological deficits following a stroke [54,55]. We did not evaluate the long-term effects of miR-29a-5p modulation on astrocyte function and neuroprotection, nor did we investigate potential side effects associated with miR-29a-5p modulation. Further research is warranted to clarify the direct interaction between miR-29a-5p and the predicted target gene of Fkbp5. Our study demonstrated that miR-29a-5p has a protective effect against HT in young adult male hyperglycemic rats. Further research is required to enhance the feasibility of linking animal models to human stroke, including studies on female subjects, older animals, and those with comorbid conditions such as hypertension, diabetes, and hypercholesterolemia, as the Stroke Therapy Academic Industry Roundtable recommends [56–58]. We can increase the likelihood of successful clinical translation by addressing these factors.

## 5. Conclusions

Our study underscores the protective role of miR-29a-5p in astrocytes under ischemia-reperfusion injury conditions. By targeting Gsk3b, Aqp4, and Fkbp5, miR-29a-5p effectively reduces astrocyte injury and fosters a neuroprotective environment. MiR-29a-5p could be a therapeutic target to minimize HT and improve outcomes following mechanical reperfusion in AIS.

## CRediT authorship contribution statement

**Chang-Luo Li:** Writing – original draft, Methodology, Investigation, Formal analysis. **Jin-Kun Zhuang:** Writing – original draft, Methodology, Investigation, Formal analysis. **Zhong Liu:** Investigation, Formal analysis. **Zhong-Run Huang:** Investigation, Formal analysis. **Chun Xiang:** Investigation, Formal analysis. **Qian-Yu Chen:** Investigation, Formal analysis. **Ze-Xin Chen:** Investigation, Formal analysis. **Zhong-Song Shi:** Writing – review & editing, Writing – original draft, Visualization, Validation, Supervision, Resources, Project administration, Methodology, Investigation, Funding acquisition, Formal analysis, Data curation, Conceptualization.

## Ethics statements

The study was reviewed and approved by the Institutional Animal Care and Use Committee of Sun Yat-sen Memorial Hospital, Sun Yat-sen University.

## Funding statement

This study was funded by the National Natural Science Foundation of

China (81720108014), the Science and Technology Planning Project of Guangzhou City (201704020166) and the Science and Technology Planning Project of Guangdong Province (2023B1212060018).

### Declaration of competing interest

The authors declare that they have no known competing financial interests or personal relationships that could have appeared to influence the work reported in this paper.

### Appendix A. Supplementary data

Supplementary data to this article can be found online at <https://doi.org/10.1016/j.ncrna.2025.05.016>.

### References

- C.B. Majoie, F. Cavalcante, J. Gralla, P. Yang, J. Kaesmacher, K.M. Treurniet, et al., Value of intravenous thrombolysis in endovascular treatment for large-vessel anterior circulation stroke: individual participant data meta-analysis of six randomised trials, *Lancet* 402 (2023) 965–974, [https://doi.org/10.1016/S0140-6736\(23\)01142-X](https://doi.org/10.1016/S0140-6736(23)01142-X).
- V. Costalat, T.G. Jovin, J.F. Albucher, C. Cognard, H. Henon, N. Nouri, et al., Trial of thrombectomy for stroke with a large infarct of unrestricted size, *N. Engl. J. Med.* 390 (2024) 1677–1689, <https://doi.org/10.1056/NEJMoa2314063>.
- T.N. Nguyen, M. Abdalkader, U. Fischer, Z. Qiu, S. Nagel, H.S. Chen, et al., Endovascular management of acute stroke, *Lancet* 404 (2024) 1265–1278, [https://doi.org/10.1016/S0140-6736\(24\)01410-7](https://doi.org/10.1016/S0140-6736(24)01410-7).
- A. Mizuma, J.S. You, M.A. Yenari, Targeting reperfusion injury in the age of mechanical thrombectomy, *Stroke* 49 (2018) 1796–1802, <https://doi.org/10.1161/STROKEAHA.117.017286>.
- Y. Zhou, Y. He, S. Yan, L. Chen, R. Zhang, J. Xu, et al., Reperfusion injury is associated with poor outcome in patients with recanalization after thrombectomy, *Stroke* 54 (2023) 96–104, <https://doi.org/10.1161/STROKEAHA.122.039337>.
- W. van der Steen, N.A.M. van der Ende, S.P.R. Luijten, L.A. Rinkel, K.R. van Kranendonk, H. van Voorst, et al., Type of intracranial hemorrhage after endovascular stroke treatment: association with functional outcome, *J. Neurointervent Surg.* 15 (2023) 971–976, <https://doi.org/10.1136/jnis-2022-019474>.
- P. Harker, Y.N. Aziz, J. Vranic, R. Chulluncuy-Rivas, M. Previtera, S. Yaghi, et al., Asymptomatic intracerebral hemorrhage following endovascular stroke therapy is not benign: a systematic review and meta-analysis, *J. Am. Heart Assoc.* 13 (2024) e031749, <https://doi.org/10.1161/JAHA.123.031749>.
- K. Suzuki, T. Katano, S. Numao, Y. Nishi, A. Kutsuna, T. Kanamaru, et al., The effect of asymptomatic intracranial hemorrhage after mechanical thrombectomy on clinical outcome, *J. Neurol. Sci.* 457 (2024) 122868, <https://doi.org/10.1016/j.jns.2024.122868>.
- S.W. Wang, Z. Liu, Z.S. Shi, Non-coding RNA in acute ischemic stroke: mechanisms, biomarkers and therapeutic targets, *Cell Transplant.* 27 (2018) 1763–1777, <https://doi.org/10.1177/0963689718806818>.
- X. Liu, L. Shen, B. Han, H. Yao, Involvement of noncoding RNA in blood-brain barrier integrity in central nervous system disease, *Noncoding RNA Res.* 6 (2021) 130–138, <https://doi.org/10.1016/j.ncrna.2021.06.003>.
- R. Han, P. Zhang, H. Li, Y. Chen, Y. Hao, Q. Guo, et al., Differential expression and correlation analysis of global transcriptome for hemorrhagic transformation after acute ischemic stroke, *Front. Neurosci.* 16 (2022) 889689, <https://doi.org/10.3389/fnins.2022.889689>.
- M.A. Neag, A.O. Mitre, C.C. Burlacu, A.I. Inceu, C. Mihu, C.S. Melincovici, et al., miRNA involvement in cerebral ischemia-reperfusion injury, *Front. Neurosci.* 16 (2022) 901360, <https://doi.org/10.3389/fnins.2022.901360>.
- Y. Liu, Y. Li, J. Zang, T. Zhang, Y. Li, Z. Tan, et al., CircOGDH is a penumbra biomarker and therapeutic target in acute ischemic stroke, *Circ. Res.* 130 (2022) 907–924, <https://doi.org/10.1161/CIRCRESAHA.121.319412>.
- X.L. Chen, Q.D. Tan, K.J. Chen, D.N. Zheng, H.W. Deng, S. He, et al., CircRNA and stroke: new insight of potential biomarkers and therapeutic targets, *Neurochem. Res.* 49 (2024) 557–567, <https://doi.org/10.1007/s11064-023-04077-6>.
- Y.B. Ouyang, L. Xu, Y. Lu, X. Sun, S. Yue, X.X. Xiong, et al., Astrocyte-enriched miR-29a targets PUMA and reduces neuronal vulnerability to forebrain ischemia, *GLIA (New York, N. Y.)* 61 (2013) 1784–1794, <https://doi.org/10.1002/glia.22556>.
- Y. Wang, J. Huang, Y. Ma, G. Tang, Y. Liu, X. Chen, et al., MicroRNA-29b is a therapeutic target in cerebral ischemia associated with aquaporin 4, *J. Cerebr. Blood Flow Metabol.* 35 (2015) 1977–1984, <https://doi.org/10.1038/jcbfm.2015.156>.
- M. Kobayashi, C. Benakis, C. Anderson, M.J. Moore, C. Poon, K. Uekawa, et al., AGO CLIP reveals an activated network for acute regulation of brain glutamate homeostasis in ischemic stroke, *Cell Rep.* 28 (2019) 979–991, <https://doi.org/10.1016/j.celrep.2019.06.075>, e6.
- B. Li, Y. Lu, R. Wang, T. Xu, X. Lei, H. Jin, et al., miR-29c inhibits TNF- $\alpha$ -induced ROS production and apoptosis in mouse hippocampal HT22 cell line, *Neurochem. Res.* 48 (2023) 519–536, <https://doi.org/10.1007/s11064-022-03776-w>.
- F. Zhao, H. Zhao, J. Fan, R. Wang, Z. Han, Z. Tao, et al., miR-29a knockout aggravates neurological damage by pre-polarizing M1 microglia in experimental rat models of acute stroke, *Front. Genet.* 12 (2021) 642079, <https://doi.org/10.3389/fgene.2021.642079>.
- Y.H. Tuo, Z. Liu, J.W. Chen, Q.Y. Wang, S.L. Li, M.C. Li, et al., NADPH oxidase inhibitor improves outcome of mechanical reperfusion by suppressing hemorrhagic transformation, *J. Neurointervent Surg.* 9 (2017) 492–498, <https://doi.org/10.1136/neurintsurg-2016-012377>.
- Z. Liu, Y.H. Tuo, J.W. Chen, Q.Y. Wang, S. Li, M.C. Li, et al., NADPH oxidase inhibitor regulates microRNAs with improved outcome after mechanical reperfusion, *J. Neurointervent Surg.* 9 (2017) 702–706, <https://doi.org/10.1136/neurintsurg-2016-012463>.
- R. Patani, G.E. Hardingham, S.A. Liddelow, Functional roles of reactive astrocytes in neuroinflammation and neurodegeneration, *Nat. Rev. Neurol.* 19 (2023) 395–409, <https://doi.org/10.1038/s41582-023-00822-1>.
- S.A. Liddelow, K.A. Guttenplan, L.E. Clarke, F.C. Bennett, C.J. Bohlen, L. Schirmer, et al., Neurotoxic reactive astrocytes are induced by activated microglia, *Nature* 541 (2017) 481–487, <https://doi.org/10.1038/nature21029>.
- C. Wang, L. Li, The critical role of KLF4 in regulating the activation of A1/A2 reactive astrocytes following ischemic stroke, *J. Neuroinflammation* 20 (2023) 44, <https://doi.org/10.1186/s12974-023-02742-9>.
- A. Lu, J.F. Clark, J.P. Broderick, G.J. Pyne-Geithman, K.R. Wagner, P. Khatri, et al., Mechanical reperfusion is associated with post-ischemic hemorrhage in rat brain, *Exp. Neurol.* 216 (2009) 407–412, <https://doi.org/10.1016/j.expneurol.2008.12.020>.
- B.A. Sutherland, A.A. Neuhaus, Y. Couch, J.S. Balami, G.C. DeLuca, G. Hadley, et al., The transient intraluminal filament middle cerebral artery occlusion model as a model of endovascular thrombectomy in stroke, *J. Cerebr. Blood Flow Metabol.* 36 (2016) 363–369, <https://doi.org/10.1177/0271678X15606722>.
- P. Liu, H. Zhao, R. Wang, P. Wang, Z. Tao, L. Gao, et al., miRNA-424 protects against focal cerebral ischemia and reperfusion injury in mice by suppressing oxidative stress, *Stroke* 46 (2015) 513–519, <https://doi.org/10.1161/STROKEAHA.114.007482>.
- A.P. Qin, C.F. Liu, Y.Y. Qin, L.Z. Hong, M. Xu, L. Yang, et al., Autophagy was activated in injured astrocytes and mildly decreased cell survival following glucose and oxygen deprivation and focal cerebral ischemia, *Autophagy* 6 (2010) 738–753, <https://doi.org/10.4161/auto.6.6.12573>.
- S. Uhlmann, E. Mracsko, E. Javidi, S. Langle, A. Teixeira, A. Hotz-Wagenblatt, et al., Genome-wide analysis of the circulating miRNome after cerebral ischemia reveals a reperfusion-induced microRNA cluster, *Stroke* 48 (2017) 762–769, <https://doi.org/10.1161/STROKEAHA.116.013942>.
- R. Wei, R. Zhang, H. Li, H. Li, S. Zhang, Y. Xie, et al., miR-29 targets PUMA to suppress oxygen and glucose deprivation/reperfusion (OGD/R)-induced cell death in hippocampal neurons, *Curr. Neurovascul. Res.* 15 (2018) 47–54, <https://doi.org/10.2174/1567202615666180403170902>.
- S. Wang, N. Li, X. Meng, Silencing of the circ-Arhgap5 RNA protects neuronal PC12 cells against injury and depends on the miR-29a-3p/Rock1 axis, *Metab. Brain Dis.* 38 (2023) 1285–1296, <https://doi.org/10.1007/s11011-023-01178-7>.
- X.Z. Gao, Z.X. Zhang, G.L. Han, miR-29a-3p enhances the viability of rat neuronal cells that injured by oxygen-glucose deprivation/reoxygenation treatment through targeting TNFRSF1A and regulating NF- $\kappa$ B signaling pathway, *J. Stroke Cerebrovasc. Dis.* 29 (2020) 105210, <https://doi.org/10.1016/j.jstrokecerebrovasdis.2020.105210>.
- H. Guo, Z. Fan, S. Wang, L. Ma, J. Wang, D. Yu, et al., Astrocytic A1/A2 paradigm participates in glycogen mobilization mediated neuroprotection on reperfusion injury after ischemic stroke, *J. Neuroinflammation* 18 (2021) 230, <https://doi.org/10.1186/s12974-021-02284-y>.
- W. Wang, M. Li, Y. Wang, Z. Wang, W. Zhang, F. Guan, et al., GSK-3 $\beta$  as a target for protection against transient cerebral ischemia, *Int. J. Med. Sci.* 14 (2017) 333–339, <https://doi.org/10.7150/ijms.17514>.
- N. Matei, J. Camara, D. McBride, R. Camara, N. Xu, J. Tang, et al., Intranasal wnt3a attenuates neuronal apoptosis through Frz1/PIWIL1a/FOXM1 pathway in MCAO rats, *J. Neurosci.* 38 (2018) 6787–6801, <https://doi.org/10.1523/JNEUROSCI.2352-17.2018>.
- K. Chen, B. Xu, S. Qiu, L. Long, Q. Zhao, J. Xu, et al., Inhibition of phosphodiesterase 4 attenuates aquaporin 4 expression and astrocyte swelling following cerebral ischemia/reperfusion injury, *GLIA (New York, N. Y.)* 72 (2024) 1629–1645, <https://doi.org/10.1002/glia.24572>.
- S. Yu, M. Yu, Z. Bu, P. He, J. Feng, FKBP5 exacerbates impairments in cerebral ischemic stroke by inducing autophagy via the AKT/FOXO3 pathway, *Front. Cell. Neurosci.* 14 (2020) 193, <https://doi.org/10.3389/fncel.2020.00193>.
- H. Kim, K. Leng, J. Park, A.G. Sorets, S. Kim, A. Shostak, et al., Reactive astrocytes transduce inflammation in a blood-brain barrier model through a TNF-STAT3 signaling axis and secretion of alpha 1-antichymotrypsin, *Nat. Commun.* 13 (2022) 6581, <https://doi.org/10.1038/s41467-022-34412-4>.
- C. Escartin, E. Galea, A. Lakatos, J.P. O'Callaghan, G.C. Petzold, A. Serrano-Pozo, et al., Reactive astrocyte nomenclature, definitions, and future directions, *Nat. Neurosci.* 24 (2021) 312–325, <https://doi.org/10.1038/s41593-020-00783-4>.
- Q. Zhang, C. Liu, R. Shi, S. Zhou, H. Shan, L. Deng, et al., Blocking C3d+/GFAP+ A1 astrocyte conversion with semaglutide attenuates blood-brain barrier disruption in mice after ischemic stroke, *Aging. Dis.* 13 (2022) 943–959, <https://doi.org/10.14336/AD.2021.1029>.
- C. Liu, Y. Guo, S. Deng, S. Zhou, S. Wu, T. Chen, et al., Hemorrhagic stroke-induced subtype of inflammatory reactive astrocytes disrupts blood-brain barrier, *J. Cerebr. Blood Flow Metabol.* 44 (2024) 1102–1116, <https://doi.org/10.1177/0271678X241235008>.

- [42] J.I. Alvarez, A. Dodelet-Devillers, H. Kebir, I. Ifergan, P.J. Fabre, S. Terouz, et al., The Hedgehog pathway promotes blood-brain barrier integrity and CNS immune quiescence, *Science* 334 (2011) 1727–1731, <https://doi.org/10.1126/science.1206936>.
- [43] S. Michinaga, S. Hishinuma, Y. Koyama, Roles of astrocytic sonic hedgehog production and its signal for regulation of the blood-brain barrier permeability, *Vitam. Horm.* 126 (2024) 97–111, <https://doi.org/10.1016/bs.vh.2024.04.006>.
- [44] G. Xing, T. Zhao, X. Zhang, H. Li, X. Li, P. Cui, et al., Astrocytic sonic hedgehog alleviates intracerebral hemorrhagic brain injury via modulation of blood-brain barrier integrity, *Front. Cell. Neurosci.* 14 (2020) 575690, <https://doi.org/10.3389/fncel.2020.575690>.
- [45] X. Ge, Z. Han, F. Chen, H. Wang, B. Zhang, R. Jiang, et al., MiR-21 alleviates secondary blood-brain barrier damage after traumatic brain injury in rats, *Brain Res.* 1603 (2015) 150–157, <https://doi.org/10.1016/j.brainres.2015.01.009>.
- [46] X. Ge, S. Huang, H. Gao, Z. Han, F. Chen, S. Zhang, et al., MiR-21-5p alleviates leakage of injured brain microvascular endothelial barrier in vitro through suppressing inflammation and apoptosis, *Brain Res.* 1650 (2016) 31–40, <https://doi.org/10.1016/j.brainres.2016.07.015>.
- [47] X. Ge, W. Li, S. Huang, Z. Yin, M. Yang, Z. Han, et al., Increased miR-21-3p in injured brain microvascular endothelial cells after traumatic brain injury aggravates blood-brain barrier damage by promoting cellular apoptosis and inflammation through targeting MAT2B, *J. Neurotrauma* 36 (2019) 1291–1305, <https://doi.org/10.1089/neu.2018.5728>.
- [48] C.M. Stary, X. Sun, Y. Ouyang, L. Li, R.G. Giffard, MiR-29a differentially regulates cell survival in astrocytes from cornu ammonis 1 and dentate gyrus by targeting VDAC1, *Mitochondrion* 30 (2016) 248–254, <https://doi.org/10.1016/j.mito.2016.08.013>.
- [49] Y. Zheng, C. Pan, M. Chen, A. Pei, L. Xie, S. Zhu, MiR-29a ameliorates ischemic injury of astrocytes in vitro by targeting the water channel protein aquaporin 4, *Oncol. Rep.* 41 (2019) 1707–1717, <https://doi.org/10.3892/or.2019.6961>.
- [50] Q. Luo, X. Xing, Y. Song, B. Gu, Q. Hu, W. Liu, et al., MiR-29a-3p ameliorate behavioral deficiency in hypoxia-ischemia brain damage in neonatal mice by inhibiting BTG2, *Behav. Brain Res.* 486 (2025) 115552, <https://doi.org/10.1016/j.bbr.2025.115552>.
- [51] X. Liu, X. Lv, Z. Liu, M. Zhang, Y. Leng, MicroRNA-29a in astrocyte-derived extracellular vesicles suppresses brain ischemia reperfusion injury via TP53INP1 and the NF- $\kappa$ B/NLRP3 axis, *Cell. Mol. Neurobiol.* 42 (2022) 1487–1500, <https://doi.org/10.1007/s10571-021-01040-3>.
- [52] Y.L. Yang, P.W. Wang, F.S. Wang, H.Y. Lin, Y.H. Huang, MiR-29a modulates GSK3 $\beta$ /SIRT1-linked mitochondrial proteostatic stress to ameliorate mouse non-alcoholic steatohepatitis, *Int. J. Mol. Sci.* 21 (2020) 6884, <https://doi.org/10.3390/ijms21186884>.
- [53] H. Shen, L. Li, S. Yang, D. Wang, S. Zhong, J. Zhao, et al., MicroRNA-29a contributes to drug-resistance of breast cancer cells to adriamycin through PTEN/AKT/GSK3 $\beta$  signaling pathway, *Gene (Amst.)* 593 (2016) 84–90, <https://doi.org/10.1016/j.gene.2016.08.016>.
- [54] J. Ruan, Y. Yao, Behavioral tests in rodent models of stroke, *Brain Hemorrh.* 1 (2020) 171–184, <https://doi.org/10.1016/j.hest.2020.09.001>.
- [55] Y. Jiang, Y. Ji, I.Y. Zhou, N. Liu, P.Z. Sun, M. Ning, et al., Effects of the new thrombolytic compound LT3001 on acute brain tissue damage after focal embolic stroke in rats, *Transl. Stroke Res.* 15 (2024) 30–40, <https://doi.org/10.1007/s12975-022-01107-3>.
- [56] M. Fisher, G. Feuerstein, D.W. Howells, P.D. Hurn, T.A. Kent, S.I. Savitz, et al., Update of the stroke therapy academic industry roundtable preclinical recommendations, *Stroke* 40 (2009) 2244–2250, <https://doi.org/10.1161/STROKEAHA.108.541128>.
- [57] M.L. Gunderson, S. Heer, A.C. Klahr, A pilot systematic review and meta-analysis of neuroprotective studies in female rodent models of ischemic stroke, *Transl. Stroke Res.* 15 (2024) 364–377, <https://doi.org/10.1007/s12975-023-01134-8>.
- [58] R.B. Patel, M. Kumskova, H. Kodali, I. Budnik, V. Kuznetsov, A. Jain, et al., Uric acid stroke cerebroprotection transcended sex, age, and comorbidities in a multicenter preclinical trial, *Stroke* 56 (2025) 965–973, <https://doi.org/10.1161/STROKEAHA.124.048748>.